Simulation Operation System of Civil Aviation Professional Electromechanical Equipment Based on Human-Computer Interaction

Dan Zhao(✉) and Xin Zhang

College of Aeronautical Engineering, Beijing Polytechnic, Beijing 100176, China
bishe16@163.com

Abstract. Traditional equipment simulation operating system adopts the principle of combining real object with simulation, which has the problems of poor feedback accuracy and slow operation feedback speed. In view of the above problems, this research designs a civil aviation professional electromechanical equipment simulation and operation system based on human-computer interaction. Taking FPGA and arm as the core, the hardware part of the system is designed by connecting Kinect sensor. After the electromechanical equipment simulation model is established by using 3D Max software, the key frames in the actual operation interactive action video are extracted by using k-means clustering algorithm, and then the simulation operation gestures are recognized by combining with the expert judgment module, so as to realize the electromechanical equipment simulation operation training under human-computer interaction. Experimental results show that the feedback accuracy of the system is higher than 95%, and the feedback is sensitive, interactive and the simulation scene is clearer.

Keywords: Civil aviation · Simulation practice of electromechanical equipment · Human computer interaction · Gesture recognition

1 Introduction

Driven by the rapid development of automation and intelligent technology, all kinds of electromechanical equipment are emerging and playing an important role in many fields. The electromechanical system of civil aviation is very complex. The use of professional electromechanical equipment requires users to invest a lot of time and energy.

Due to the complexity of the structure and operation of civil aviation professional electromechanical equipment, operators need to spend a lot of time learning during the training operation of civil aviation professional electromechanical equipment, and the operation process is not monitored, and it is difficult to control errors [1]. In addition, in the practical operation of civil aviation professional electromechanical equipment, due to the high cost of equipment and consumables, the shortage of equipment and tools, and the danger of operation to newly trained personnel, the practical operation efficiency is very low. Therefore, the operation practice of professional electromechanical equipment

W. Fu and G. Sun (Eds.): eLEOT 2022, LNICST 453, pp. 737–750, 2022.
https://doi.org/10.1007/978-3-031-21161-4_56

assisted by the actual operation simulation system can reduce the improper damage to the equipment or the impact on personnel safety during the actual operation of the equipment.

At present, the practice system of electromechanical equipment in civil aviation specialty mainly uses electromechanical equipment model and training prototype for modular training, or learns and operates through computer simulation system under the guidance of teaching personnel after learning relevant theories. The system combining physical object and virtual platform in reference [2] reduced the cost investment to a certain extent. However, with the continuous development and maturity of virtual reality technology, integrating virtual reality technology into the virtual operation process of civil aviation professional electromechanical equipment obviously has more important practical significance for cultivating professional students' practical operation ability and reducing training operation cost. Therefore, reference [3] designed a practical operation system based on virtual reality, which improves the students' practical operation efficiency of diesel engine. However, when virtual reality technology is applied to the practical operation simulation system of civil aviation electromechanical equipment, the interaction with system users is poor, lack of realism, and the real-time performance of the system is poor.

The emergence and development of human-computer interaction technology provides a new idea for the practical operation of aviation electromechanical equipment. This new interaction technology can provide a new interactive experience in the teaching and training of electromechanical equipment of civil aviation specialty, and can also provide technical assistance for operators by using a new display mode, which can effectively reduce human errors in the process of practical operation, reduce the probability of wrong operation during real operation and avoid damage to civil aviation professional electromechanical equipment.

According to the above research and analysis contents, in order to improve the talent training speed of civil aviation and improve the familiarity and mastery of civil aviation professional electromechanical equipment, this paper will design a civil aviation professional electromechanical equipment simulation and operation system based on human-computer interaction. Through the application of the system, the training conditions can be improved in the training teaching, and the human-computer interaction can be realized assemble the accessories in the virtual environment to reduce the operational risk in the practical operation of aviation special electromechanical equipment and improve the skill level of learners.

2 System Hardware Design

The hardware structure of the simulation practical operation system of civil aviation professional electromechanical equipment based on human-computer interaction is shown in Fig. 1.

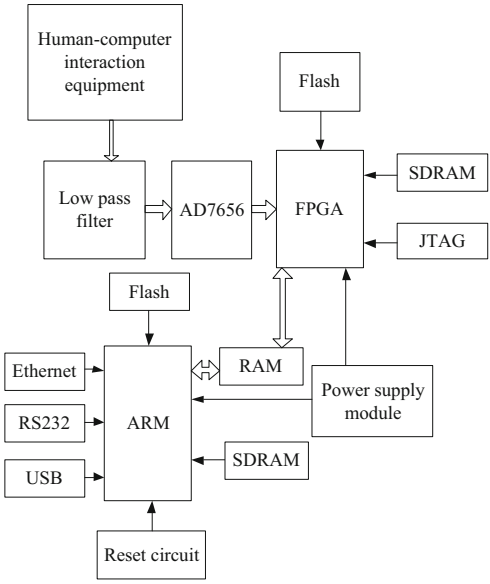

Fig. 1. Schematic diagram of the overall system hardware architecture

In Fig. 1, the embedded real-time operating system is located at the core. As the logic processing unit of the whole system, the core unit has network interface, ARM hardware and FPGA, and has the function of real-time multitasking.

According to the analysis of the human-machine function requirements of the simulation actual operation system, the human-machine application layer mainly realizes the functions of file input and output, parameter setting and running status monitoring. Users can intuitively observe the operating status of the equipment and find problems through the human-machine application layer And the operation to deal with emergencies [4]. The ARM hardware platform uses Samsung S3C6410 as the core processor to implement hardware support for embedded Linux systems and hardware support for data communication. Select through the OM[I:O] pin. When OM[1:0] = 00, the processor will boot from NAND Flash; when OM[1″0] = 01 or 10, the processor will boot from ROM [5]. Peripheral The human-computer interaction interface mainly includes USB interface, LCD interface, keyboard interface, touch screen interface and SD card interface, which mainly realizes the input and output of files and data, as well as data storage.

The voltage conversion circuit mainly uses the ACT6311 power conversion chip and the +10 V, +16 V, −7 V and +3.7 V voltages of the LM358DR. The parameter acquisition module is responsible for converting the strong electric signal generated by the human-computer interaction device into a weak electric signal suitable for AD sampling. It consists of a voltage acquisition circuit, a current acquisition circuit, a low-pass filter circuit, a frequency measurement circuit, and a phase-locked frequency multiplication circuit. The filtered signal is sent to the analog signal input end of AD7656 through a voltage follower for AD conversion. The AD sampling module samples the

six signals output by the parameter acquisition module through the externally expanded AD7656 chip [6]. The phase-locked frequency multiplication circuit is used to obtain a square wave signal with 256 times the frequency of the input signal as the driving pulse for AD sampling, so that it can ensure that the AD converter can sample 256 points per cycle. The FPGA will lose its configuration every time it is powered down, so every time it is powered on, it needs to load the startup code from the external storage. The CY22394 clock generator from CYPRESS is used. The chip integrates three programmable phase-locked loops and independently outputs 4 channels of 2000 MHz clock signals.

The data communication of the system is mainly based on dual-port RAM, supplemented by serial communication. Among them, dual-port RAM is mainly used for the communication between the upper computer and the lower computer, and RS232 is mainly used for the communication between the upper computer and the PC. The main function is to print information of the system and serve as the debugging serial port of the system and the man-machine. RS485 mainly realizes the input of keys and can also be used as a data communication interface between the upper computer and the lower computer. In order to improve the scalability and versatility of the system and realize the distributed control, this article uses Ethernet as another method of data communication. The communication in this article mainly adopts the format of the virtual sCAN protocol, encapsulating the source address, destination address, instruction code, function code and function parameters into a data frame to realize the communication between the upper computer and the lower computer. The definition of the communication data frame format is shown in Table 1.

Table 1. System communication data frame format definition

Data frame bit number	Address	Transfer content
1	Ad0	Script
2	Ad1	Function code
3	Ad2	Data1
4	Ad3	Data2
5	Ad4	Data3
6	Ad5	Data4
7	Ad6	Data5
8	Ad7	Data6
9	Ad8	Data7
10	Ad9	Data8
11	Ad10	Request code/response code

In order to improve the realism and interactivity of using the system for the practical operation of civil aviation professional electromechanical equipment, the system uses the Kinect somatosensory device to capture the operation of the system user. The internal

processor chip of the Kinect sensor selected in this design is PS1080, which can process the reflected speckle image collected by the infrared camera and generate depth and distance information.

The main sensor parameters of Kinect sensing equipment are shown in Table 2.

Table 2. Kinect sensor equipment parameters

Numbering	Sensor parameters	Parameter data
1	Measurable distance	0.8–4 m
2	Visual field	Vertical: 45°; Horizontal: 55°
3	Frame rate	50 fps/s
4	Depth camera	720 * 480
5	Color camera	1280 * 1080

Through the setting of the above parameters, the Kinect sensor can collect 3D data of each joint point of human motion in real time for modeling. Through the difference between the angle and depth of each joint and the fingertip of the limb, the posture of the human body can be judged, and the position of each node can be determined at the same time. Time difference to track the direction of human body movement.

In the process of human-computer interaction, DS90CR288A is selected as the chip to decode the operator's behavior image. The chip supports up to 85 MHz clock and the maximum transmission bandwidth of the chip is up to 100 Mbps [7]. The image data is converted in real time through the PCI-E interface for data transmission. In order to ensure the PCI-E transmission efficiency and increase the transmission bandwidth, the extended DDR3 SDRAM is used to cache the data. Expand all data and control signals of DDR3 through BANK34.

With the support of the above-designed system hardware framework, design the software part of the simulation and actual operation system of civil aviation professional electromechanical equipment to realize the use of system design functions.

3 System Software Design

3.1 Simulation Modeling of Electromechanical Equipment

When users use the civil aviation professional electromechanical equipment simulation practical operation system based on human-computer interaction for practical exercises, the system needs to have the correct civil aviation electromechanical equipment model and corresponding parameters. Therefore, this article uses 3D MAX software to establish a professional electromechanical equipment model for civil aviation.

According to the geometric dimensions of the electromechanical equipment, use the standard primitives in the 3D MAX software, such as spheres, cylinders, cubes, etc., to select the corresponding standard primitives. The size is basically the same as the actual object, and the unit is millimeters. After the basic standard body is created, adjust the

length, width and height according to the actual size [8]. Super Boolean objects combine two or more other objects by performing Boolean operations. Super Boolean adds a large number of functions to the traditional 3D MAX Boolean object, using different Boolean operations, the ability to combine multiple objects at once to get mesh smoothing and turbo smoothing effects.

In actual modeling, by transforming into editable objects, taking editable polygons as an example, 3D MAX provides different levels of modification tools from vertices to elements. When building a complex model, a simple cube can be used to continuously modify its vertices, edges or polygons to create a variety of complex graphics. According to the actual material and texture characteristics of electromechanical equipment, the established model is processed in detail. According to the design parameters and related basic principles of the professional electromechanical equipment for civil aviation, the operation of the electromechanical equipment model is expressed by mathematical simulation, so that the subsequent use of the system for actual operation can obtain correct feedback.

3.2 Key Frame Extraction

The user carries out the interactive action of simulation and practical operation through the camera and civil aviation professional electromechanical equipment. The key frame in the camera imaging video reflects the key video information in the video. Therefore, before practical operation recognition, this study uses K-means clustering algorithm to extract key frames.

K-means algorithm is the most widely used clustering analysis algorithm because of its simple principle, easy implementation, good clustering effect and fast convergence speed. In this paper, for 25 bone points in the action video collected by Kinect V2, combined with the cognition of human motion, weighted k-means algorithm is used to extract key frames.

In human motion, the positions of different bone points are different. For example, the weight of spine points is greater than that of wrist points, and the swing range of wrist points is larger in action, which will interfere with the cluster center. For different weights of each bone point in motion, the weight of bone point is defined according to formula (1):

$$B_i = B_i \left(\sum_{i=1}^{n} B_i \right)^{-1} \tag{1}$$

where,

$$B_i = \frac{\sum_{i=1,j=1}^{n} dist(a_i, b_j)}{n} \tag{2}$$

where, $dist(a_i, b_j)$ is the Euclidean distance between a_i and b_j. The closer the distance is, the smaller the weight is. Otherwise, it is the opposite.

In the user's practical action video collected by Kinect V2, each frame image contains the three-dimensional coordinate values of 25 bone points of the human body to form a 75 dimensional vector. An action sequence consists of N frame images, expressed as $\{p_1, p_2, \ldots, p_{n-1}, p_n\}$. p_i represents the i-th frame in the N-frame image, and P^N represents the vector set of an action video composed of 75 dimensional vectors per frame. The vector set P^N cluster is divided into K clusters, and the frame similarity in each cluster is high. The specific steps are as follows:

Step 1: randomly select K frames from the P^N frame set as the clustering centroid, representing $c_1, c_2, \ldots, c_k, k \leq N$. According to the following formula, the Euclidean distance between p^i and K cluster centroids in each frame is calculated and classified into the corresponding cluster of the nearest cluster centroid.

$$D_i = \arg\min \left\| p_i - c_j \right\| \tag{3}$$

Step 2: update the weighted average clustering centroid of each cluster according to the following formula:

$$c_j = \frac{\sum_{i=1}^{n} B_i \gamma_{ij} p_i}{\sum_{i=1}^{n} \gamma_{ij}} \tag{4}$$

where, B_i represents the weight of the data object in cluster c_j; γ_{ij} is the standard for judging whether p_i belongs to class j. If yes, the value of p_i is 1, otherwise it is 0.

Step 3: repeat steps 2 and 3 until the old and new centroids are equal or the difference is less than the threshold.

Through the above steps, a segment of electromechanical equipment operation video is divided into K clusters, and the cluster quality c_i of each cluster is obtained. Each frame in the action video is composed of 75 feature vectors with the three-dimensional coordinates of 25 bone points. Calculate the Euclidean distance between the cluster centroid and the three-dimensional coordinate value of the frame 7 {same bone point in the action sequence, and find the key frame. For example, calculate the Euclidean distance between the bone point L and the bone point l of the cluster centroid, and so on. The bone point with the smallest distance value is marked as l, and the others are marked as 0. If the frame p_i in the video passes, the calculation result is {1,l, 0, 0, 0, 0, 0, 1, l, 1, 11, l, 1, l, l, 0, 0, 01, l, l, 0, 0, 1}.

The specific steps are as follows:

Step 1: use k-means algorithm to obtain K clustering centroids of an action sequence, expressed as:

$$\begin{aligned} &B_i = \left\{(x_{i1}, y_{i1}, z_{i1}), (x_{i2}, y_{i2}, z_{i2}) \ldots, \left(x_{ij}, y_{ij}, z_{ij}\right)\right\} \\ &i \in (1, 2, \cdots, k), j = 25 \end{aligned} \tag{5}$$

where, $\left(x_{ij}, y_{ij}, z_{ij}\right)$ is the three-dimensional coordinate of the j-th bone point in the i-th cluster centroid. A continuous electromechanical equipment operation video is shown as:

$$P_n = \left\{(x_{n1}, y_{n1}, z_{n1}), (x_{n2}, y_{n2}, z_{n2}) \ldots, \left(x_{nj}, y_{nj}, z_{nj}\right)\right\}$$

$$n \in (1, 2, \cdots, N), j = 25 \tag{6}$$

where, (x_{nj}, y_{nj}, z_{nj}) represents the three-dimensional coordinates of the j-th bone node in frame n of the action video.

Step 2: calculate the Euclidean distance between the cluster centroid B_i and the three-dimensional coordinates of the 25 bone points corresponding to the operation in frame n of the action video.

After calculating the distance for each frame in the action video, mark the minimum $dis\left[(x_{ij}, y_{ij}, z_{ij}), (x_{nj}, y_{nj}, z_{nj})\right]$ as l, otherwise mark it as 0.

The minimum Euclidean distance of key points corresponding to each frame and K clustering centroids is obtained through the Euclidean distance formula, and the first K frames are selected as key frames according to the number of l in B, and then sorted according to the index of each key frame in the original action video, so as to ensure that the order of K key frames is consistent with that in the action video.

The k-means algorithm is used to obtain the effective and key image information in the actual operation video of aviation professional electromechanical equipment, in which the selection of K value is also the key part. The K value is small, the information obtained is too small, and the recognition accuracy is low; When the K value is large, there is more redundant information, and the recognition accuracy will also be affected. In this paper, when the K value is set to 10, better accuracy and recognition speed can be obtained.

3.3 Practical Gesture Recognition of Electromechanical Equipment

The gesture area is extracted from the depth image obtained by the Kinect sensor, and the number of fingers is recognized and compared with the preset number of gesture fingers to realize the recognition of gestures and complete the algorithm framework of static gesture recognition.

First, establish the coordinate transformation of the operator's gesture in the Kinect sensor, the human-computer interaction device and the space. The coordinate of the hand coordinate system is $\{H\}_r^l = \{X_H, Y_H, Z_H\}$, the coordinate of the hand in the space coordinate system is $\{P\}_r^l = \{X_P, Y_P, Z_P\}$, and the coordinate of the hand in the human-computer interaction device coordinate system is $\{W\}_r^l = \{X_W, Y_W, Z_W\}$. According to the posture of the gesture in different coordinate systems, combined with the law of rotation, the position ${}^{Y}HP$ and posture of the hand in the applied coordinate system are obtained:

$${}^{Y}HP = \left(\{H\}_r^l\{P\}_r^l + \alpha\right)\{W\}_r^l + \{W\}^l \tag{7}$$

$$\{Z\}_r^l = \alpha\beta\{W\}_r^l \tag{8}$$

In the formula, α and β are respectively the rotation and translation amount of the applied coordinate system relative to the hand coordinate system. After determining the coordinates of the gesture in the image, segment the gesture area. When the image depth value is in the range of 600 ~ 800, the recognition rate is significantly improved, and the value is relatively stable; after the depth value reaches 800, the recognition rate begins

to decrease; when the depth value is between 700 and 900, the recognition rate can reach more than 90%; depth value When it is greater than 900, the recognition rate drops significantly [9]. Considering that in the process of gesture recognition, the distance between the hand and the device will change to a certain extent, so this article uses 700 to 800 as the depth range threshold. The K-Means algorithm is used to complete the next segmentation of the gesture area. The purpose of gesture area filtering and morphological operations is to remove noise in the image and fill in some small holes, so as to better retain the edge information of the object.

In this paper, the traditional median filter is improved, and the calculation is simplified by removing only the zero-value noise points. First define the filtering window, this article uses a 5×5 neighborhood window. According to the center value of the window, it is judged whether it is a value of 0, if it is not a value of 0, no processing is done; if it is a value of 0, all pixels with a value of 0 in the window are removed, and the remaining pixel values are searched for the median value as The center point of the window effectively filters out the noise in the image. If the gray value of a pixel (x, y) in the image is $f(x, y)$. The window size of the median filter is 5×5. When the window moves to the vicinity of pixel (x, y), the gray value of the center pixel of the window can be used to replace the gray value of all pixels in the window [10]. Then the pixel gray value of the median filter window can be sorted by the following formula:

$$\{F_{i-v}, \cdots, F_{i-1}, \cdots, F_i, F_{i+1}, \cdots, F_{i+v}\} \tag{9}$$

In the formula, F_i is the output of the median filter, $v = L - 1/2$ and L are the width of the median filter window. After the image to be recognized is processed by the median filter, the noise generated by the external interference during the image acquisition and conversion process can be removed. In this paper, the threshold is set according to the difference of V (brightness) in HSV. If the difference of V is less than 100, the pixel is set to black; when V is greater than 100, the pixel is set to white. Next, scan each pixel point in sequence from different directions; if the value is different from the adjacent two pixels on the left and right, the point is regarded as the boundary point, and the process is looped to find the contour of the gesture.

The depth image obtained by Kinect calculates the three-dimensional coordinate information of each bone point of the human body, thereby calculating the moving distance of each bone point in the two images before and after. If the distance is less than the preset threshold, it is judged as a static state, which means that it is the same action. The distance between the bone points in the two images before and after the detection is phased, including the start point and the end point. Therefore, it is very important to determine the start and end of the gesture. In the process of dynamic gesture recognition, the researcher first randomly selects the Euclidean distance of the hand points of the two images before and after. If the continuous M (M is greater than or equal to 5) images are in a static state, the next M + 1 image starts When moving, the M + 1 image is judged as the initial action of the dynamic gesture; if the continuous motion is N (N is greater than or equal to 10), the N + 5th image is in a static state until the N + 1 image value, The M + Nth image is judged to end the action.

The GetHandState function included in the Kinect SDK can be used to determine when the operator's hands are in a fisted state. In order to better determine the start of

the gesture and reduce the constraints on people, this method adds a fisted state, that is, when the operator's hands are in a fisted state. When the hand is in a fisted state, the discrimination method becomes effective. Proceed as follows:

1) Call the GetHandState() function to judge whether the operator's hand is in a fisted state, if it is in a fisted state, continue to judge; otherwise, re-check whether it is in a fisted state;
2) Determine whether the M continuous images containing the hand are greater than or equal to 5 and are in a static state, and the hands are all in a fisted state, if yes, proceed to the next step of judgment; otherwise, re-detect the images;
3) Determine whether the N images containing continuous hand movement are greater than or equal to 10 and the hand is in a fisted state. If so, determine the Mth image as the start and M + N images as the end; otherwise, return to step 1.

The use of hidden Markov model needs to meet the following three premise assumptions:

1) The state has nothing to do with time;
2) The observed value at any time is only related to the current hidden state;
3) The current state is only related to the previous state.

Assuming that the parameters in the HMM and the observation sequence of the gestures are known, a matching HMM model needs to be found, and the corresponding gesture is the recognized gesture. The Baum-Welch algorithm is used to train a large number of gesture samples, and the result is the gesture corresponding to the unknown gesture.

Naive Bayes regards the dynamic behavior characteristics of different hands as independent of each other. According to Bayesian theory, there are:

$$P(a_i)P(a|b_i) = P(a_i)\prod_{j=1}^{n} P\left(b_j|a_i\right) \tag{10}$$

In the formula, b_j is the characteristic attribute of hand dynamic behavior; a_i is the characteristic of hand dynamic behavior to be classified.

Follow the flowchart shown in Fig. 2 to train and recognize gesture recognition.

The set gesture discrimination expert module is used to judge the operation of the recognized gesture, so as to guide the user to carry out the simulation operation of electromechanical equipment. Transplant the operation simulation software part designed above to the system hardware framework, that is, complete the design and research of civil aviation professional electromechanical equipment simulation operation system based on human-computer interaction.

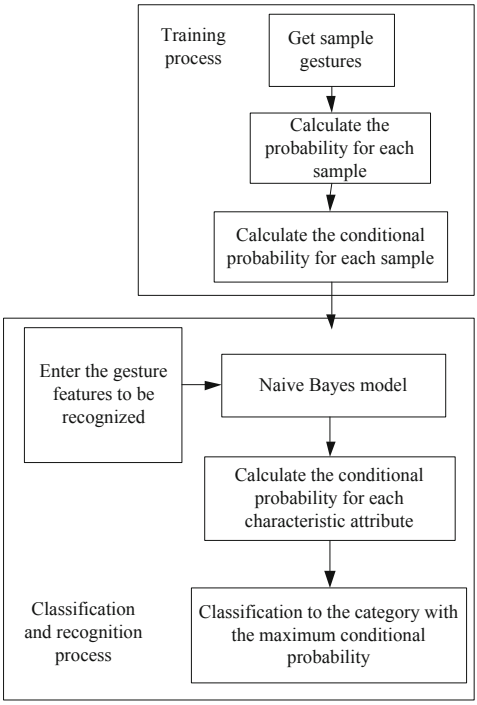

Fig. 2. Naive Bayes training and recognition process

4 Test Experiment

In order to ensure the stable operation of the system, it is necessary to test the civil aviation professional electromechanical equipment simulation operation system based on human-computer interaction.

4.1 Experiment Content

A stable hardware platform is the basis for the realization of system functions. First, the hardware platform needs to be tested, which includes the basic power on debugging, power timing quality testing and key signal testing of the system. Then, the software and hardware functions are jointly debugged; Finally, the power consumption test is carried out. System debugging requires defect detection system circuit board, power supply, serial port and network connected with debugging computer, oscilloscope, multimeter and other test tools. After confirming that all aspects of the system operate normally, conduct performance test on the system.

In the system performance test, the system designed in this paper is compared with the traditional mechanical and electrical equipment operation system. The actual power consumption, operational feedback speed, feedback accuracy and simulation scene clarity were taken as indexes to compare the application performance of the two systems. The actual power consumption of the system is reflected by the clock test result.

4.2 Experimental Results

Table 3 shows the result data of the system's clock test when testing the operation of the designed system hardware platform.

Table 3. System hardware clock test results

Signal	Theoretical clock frequency/MHz	Actual system power clock measurement value/MHz	Signal duty cycle
Signal-1	300	298.75	0.5212
Audio-25	25	24.62	0.4961
RTC_CLK	35.754	35.051	0.4798
Signal-12	12	12.00	0.5103
ETH_S	12.88	11.98	0.5044
Signal-Y	45	44.63	0.4876

According to the data analysis in Table 3, the actual measured clock frequency of system operation is close to the theoretical clock frequency. Moreover, the duty cycle of the clock signal also meets the operation requirements of the actual system.

After the system hardware test is normal, the comprehensive performance of the system is tested. Invite the same number of students to use the two systems to test the operation feedback speed, feedback accuracy and actual power consumption of the system under different use scenarios.

Figure 3 shows the comparison results of operation feedback speed and feedback accuracy of the system.

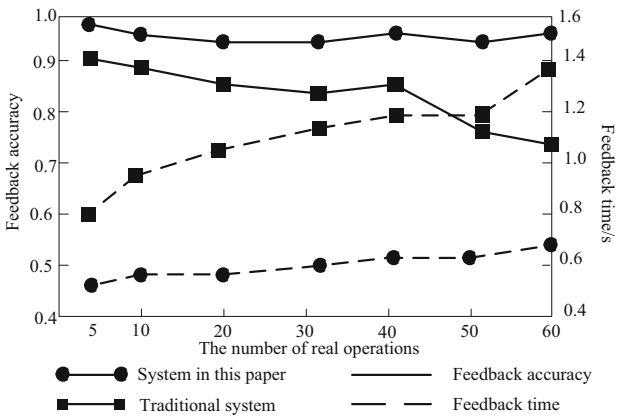

Fig. 3. Comparison of system feedback speed and accuracy

By analyzing the data in Fig. 3, it can be seen that the operation feedback speed of the system in this paper is always higher than that of the traditional system. With the

increase of the use time and operation complexity of the system, the operation feedback accuracy of the traditional system continues to decline. The operation feedback accuracy of this system is higher than 95%.

Finally, the application performance of the two systems is verified with the simulation scene clarity as an indicator, and the results are shown in Fig. 4.

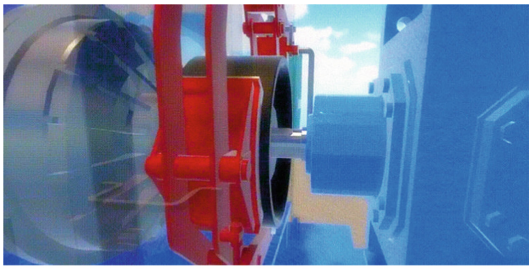

System in this paper

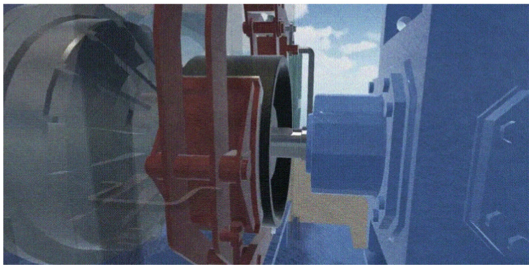

Traditional system

Fig. 4. Contrast the sharpness of simulation scenes

The results shown in Fig. 4 show that compared with the simulation scene images of traditional systems, the simulation scene images of this system have higher color saturation and clarity and better simulation effect.

By summing up the above experimental analysis, it can be judged that the simulated real operation system of civil aviation mechanical and electrical equipment based on human-computer interaction designed in this paper has good practical application performance.

5 Conclusion

The practical operation of professional electromechanical equipment for civil aviation has the problems of long preparation time, difficulty in carrying out, and many dangerous steps and procedures. Based on the virtual reality platform to carry out safe operations, set up the error operations that are easy to occur during the actual operation in the virtual environment, and combine the human-computer interaction technology to help students carry out the simulation actual operation, improve the sense of reality, and reduce the

investment and the risk of actual operation. For this reason, this paper designs a simulation and practical operation system for civil aviation professional electromechanical equipment based on human-computer interaction.

This study takes FPGA and ARM as the core, and designs the hardware part of the system by connecting Kinect sensor. After establishing the simulation model of mechanical and electrical equipment with 3D MAX software, the key frames in the interactive action video of real operation are extracted, and then the gestures of simulated operation are recognized, so as to realize the real operation training of mechanical and electrical equipment under human-machine interaction. Through the system functional test, it is verified that the system has good interactivity. It can select the practical links and difficulties according to the actual situation, and ensure the training effect of the students through the implementation of multiple simulation training.

In the following research, we will consider the introduction of graph neural network to further improve the recognition effect of simulated operation gestures.

Fund Project. Scientific research project of Beijing Polytechnic, project name: Simulation Operation System of Civil Aviation Professional Electromechanical Equipment Based on Human-Computer Interaction.

References

1. Zhou, Y., Chen, L., Wang, X., et al.: Outlook on digital intelligence aviation electromechanical technology. J. Sichuan Ordnance **42**(05), 14–19 (2021)
2. Liu, N.: Design of extensible data acquisition system for semi-physical fully mechanized mining operating platform. Ind. Mine Autom. **46**(01), 95–99 (2020)
3. Li, H., Lu, P., Li, M.: Design and implementation of virtual reality training system of a diesel engine. Comput. Simul. **36**(12), 267–271 (2019)
4. Han, Z., Yue, W.: Modelling & simulation of system reliability and maintenance cost for electromechanical equipment. Mach. Tool Hydraul. **49**(02), 110–112+116 (2021)
5. Hao, Y., Dai, X., Cui, X.: Design of integrated modular avionics architecture avionic system flight management module. Sci. Technol. Eng. **21**(16), 6923–6929 (2021)
6. Zhao, Y., Wu, T., Gu, S., et al.: Multi-index quantitative evaluation model of gunner's operation posture based on human-machine simulation technology. Comput. Integr. Manuf. Syst. **27**(08), 2350–2361 (2021)
7. Wang, J., Guan, S., Lei, M., et al.: Modeling and simulation of master manipulator based on the remote center motion mechanism. Mech. Electr. Eng. Mag. **36**(02), 179–184 (2019)
8. Cheng, R., Huang, P., Liu, Z., et al.: A human-robot interaction method of on-orbit service-oriented space teleoperation. J. Astronaut. **42**(9), 1187–1196 (2021)
9. Song, Y., Fei, Y., Sun, G., et al.: Immersive three-dimensional simulation and visualization of microelectromechanical systems. J. Syst. Simul. **26**(09), 1956–1960+1968 (2014)
10. Zhang, Y., Chang, Q., Wang, D., et al.: Research and development of 3D simulation training system for basic skills of electric energy metering device. Autom. Instrum. (04), 204–207 (2019)